Journal of Physics: Conference Series

PAPER • OPEN ACCESS

Probing asymmetric clusters by using isoscalar monopole and dipole transitions

To cite this article: M Kimura *et al* 2017 *J. Phys.: Conf. Ser.* **863** 012024

View the article online for updates and enhancements.

Related content

- Asymmetric cluster structure and isoscalar monopole/dipole transitions of 28Si
  Y Chiba, Y Taniguchi and M Kimura
- 2 + t cluster state in ^{11}B
  T Kawabata, H Akimune, H Fujita et al.
- DO VOIDS CLUSTER?
  S. Haque-Copilah and D. Basu

This content was downloaded from IP address 131.169.5.251 on 15/02/2018 at 12:55

IOP Conf. Series: Journal of Physics: Conf. Series **863** (2017) 012024 doi:10.1088/1742-6596/863/1/012024

Probing asymmetric clusters by using isoscalar monopole and dipole transitions

M Kimura[1], Y Chiba[1] and Y Taniguchi[2]

[1]Department of Physics, Hokkaido University, 060-0810 Sapporo, Japan.
[2]Department of Medical and General Sciences, Nihon Institute of Medical Science, Moroyama, Saitama 350-0435, Japan.

E-mail: masaaki@nucl.sci.hokudai.ac.jp

Abstract. The isoscalar monopole and dipole transitions and their relationship to the clustering are discussed. By exploiting the Bayman-Bohr theorem, analytical formulae for the transition matrices are derived to show that the cluster states are very strongly populated by the IS monopole and dipole transitions. For the quantitative discussion, the AMD calculations for ^{20}Ne, ^{44}Ti and ^{24}Mg are presented. It is demonstrated that IS monopole and dipole transitions are excellent probe for the clustering.

1. Introduction

At the time when K. Wildermuth, the founder of this conference series, started his study of nuclear clustering [1, 2], the concept of the nuclear clustering and the cluster models were criticized [3]. It was shown that an $SU(3)$ shell model [4] and a cluster model wave functions are mathematically equivalent to each other at the zero inter-cluster distance [3, 5], which is known as the Bayman-Bohr theorem. The theorem was misinterpreted to argue that the cluster model was not describing new aspects of atomic nuclei but just describing a known shell model state.

Today, almost 60 years later, it is interesting to know that the theorem is commonly accepted in an opposite meaning; it is one of the essential and useful theorem for the understanding of nuclear clustering. An interesting and important application of the theorem is the discussion of the isoscalar (IS) monopole and dipole transitions and their relationship to the nuclear clustering [6, 7, 8, 9, 10], which we shall discuss in this contribution.

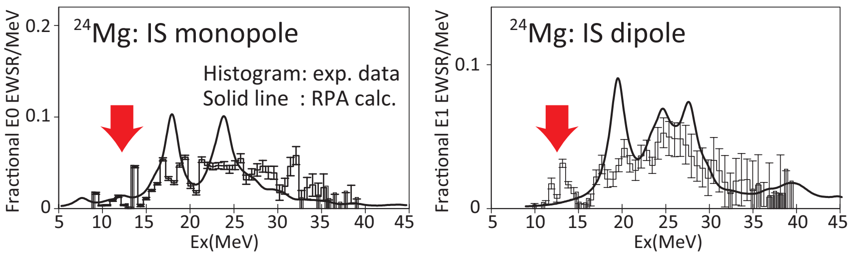

Figure 1. IS monopole and dipole strengths of ^{24}Mg. Histogram shows the experimental data, while the solid line shows the results of RPA calculation.

Content from this work may be used under the terms of the Creative Commons Attribution 3.0 licence. Any further distribution of this work must maintain attribution to the author(s) and the title of the work, journal citation and DOI.
Published under licence by IOP Publishing Ltd

Figure. 1 shows the IS monopole and dipole strengths of ^{24}Mg [14]. We see that several resonances are observed in the low energy region of $E_x = 10 \sim 15$ MeV (histograms) which are not explained by the RPA calculation (solid lines). We can also find that similar resonances are systematically observed in stable nuclei from ^{12}C to ^{40}Ca [11, 12, 13, 14, 15, 16, 17, 18]. The Bayman-Bohr theorem plays a central role to show that *they are cluster states*. With the help of the theorem, we can prove that the IS monopole and dipole transitions strongly populate cluster states, and hence, they are excellent probe for nuclear clustering. To illustrate it, we first discuss the duality of shell and cluster, and derive analytic formula for transition matrices. For the quantitative discussion, we also present the antisymmetrized molecular dynamics (AMD) calculations for ^{20}Ne, ^{44}Ti and ^{24}Mg [10, 19, 20, 21].

2. Duality of shell and cluster, and IS monopole/dipole transitions

As mentioned above, the Bayman-Bohr theorem states the equivalence of an $SU(3)$ shell model and a cluster model at the zero inter-cluster distance. For example, the shell model wave function for the ^{20}Ne ground state is equivalent to an $\alpha + {}^{16}$O cluster model wave function,

$$\Phi(0^+_1) = \mathcal{A}\left\{ (0s)^4(0p)^8(1s0d)^4 \right\}^{J^\pi=0^+}_{(8,0)} = n_{N_0}\mathcal{A}\left\{ R_{N_0 0}(r)Y_{00}(\hat{r})\phi_\alpha\phi_{\rm O} \right\}, \quad N_0 = 8 \tag{1}$$

where the inter-cluster motion between α and ^{16}O clusters is described by a harmonic oscillator wave function $R_{N_0 0}(r)Y_{00}(\hat{r})$. In this way, the theorem tells us that the ground states of atomic nuclei have duality of shell and cluster; they are two-faced like Janus. The correct interpretation of this duality is this: The degrees-of-freedom of cluster excitation is embedded even in an ideal shell model state. Hence, the pronounced cluster states can be populated from the shell model state. For example, by increasing the nodal quantum number of the inter-cluster motion, we get a wave function for an excited 0^+ state,

$$\Phi(0^+_{ex}) = \sum_{N=N_0+2}^{\infty} f_N n_N \mathcal{A}\left\{ R_{N0}(r)Y_{00}(\hat{r})\phi_\alpha\phi_{\rm O} \right\}, \tag{2}$$

which has pronounced clustering owing to the increased inter-cluster distance. Another excitation mode is the increase of the orbital angular momentum of inter-cluster motion, that yields a 1^- state with pronounced clustering,

$$\Phi(1^-_{ex}) = \sum_{N=N_0+1}^{\infty} g_N n_N \mathcal{A}\left\{ R_{N0}(r)Y_{10}(\hat{r})\phi_\alpha\phi_{\rm O} \right\}. \tag{3}$$

We call these cluster excitations “nodal” and “angular” excitations as shown in Fig. 2. In ^{20}Ne, the 0^+_4 and 1^-_1 states at 8.7 MeV and 5.8 MeV are identified as these excited states [22]. Thus, the Bayman-Bohr theorem guarantees that the pronounced cluster states can be populated from the shell model state by activating the degree-of-freedom of cluster excitation.

Now, it must be emphasized that the IS monopole/dipole transitions do realize it. They induce nodal and angular excitations to populate cluster states strongly. It is proved as follows. Using the cluster coordinate defined in Fig. 3, the IS monopole operator is rewritten as[9],

$$\mathcal{M}^{IS0} = \sum_{i=1}^{A} (\boldsymbol{r}_i - \boldsymbol{r}_{\rm cm})^2 = \sum_{i\in C_1} \xi_i^2 + \sum_{i\in C_2} \xi_i^2 + \frac{C_1C_2}{A}r^2. \tag{4}$$

Note that this expression makes it clear that $\mathcal{M}^{\rm IS0}$ will generate nodal excited states, because the last term proportional to r^2 will induce the nodal excitation of the inter-cluster motion. By a similar calculation, one finds that the isoscalar dipole operator is rewritten as [10],

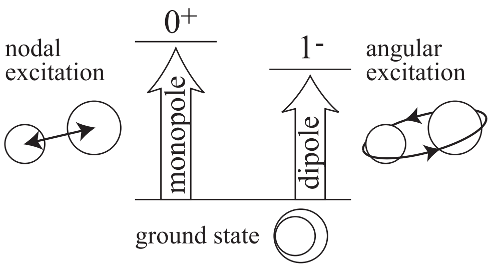

Figure 2. IS monopole and dipole transitions populate nodal and angular excited states.

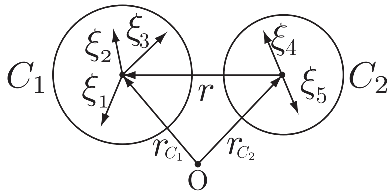

Figure 3. $\boldsymbol{\xi}_i$ denote the internal coordinates, while $\boldsymbol{r}$ is the inter-cluster coordinate. C_1 and C_2 are the masses of clusters.

$$\mathcal{M}^{IS1}_\mu = \frac{5}{3}\left(\frac{C_2}{A}\sum_{i\in C_1}\xi_i^2 - \frac{C_1}{A}\sum_{i\in C_1}\xi_i^2\right)\mathcal{Y}_{1\mu}(\boldsymbol{r}) + \frac{C_1C_2(C_1-C_2)}{A^2}r^2\mathcal{Y}_{1\mu}(\boldsymbol{r}) + ..., \tag{5}$$

where the terms depending on $\mathcal{Y}_{1\mu}(\boldsymbol{r})$ will increase the angular momentum of inter-cluster motion to generate angular excited cluster states. We also see that $\mathcal{M}^{IS1}_\mu$ is amplified for asymmetric cluster systems [23], because those terms depend on the mass asymmetry $(C_1 - C_2)/A$.

Thanks to the Bayman-Bohr theorem, it is possible to derive analytic formulae for these transition matrix by using Eqs. (1)-(5) [9, 10]. In the case of ^{20}Ne, they read

$$M^{IS0} = \langle\Phi(0^+_{ex})|\mathcal{M}^{IS0}|\Phi(0^+_{gs})\rangle = f_{N_0+2}\sqrt{\frac{\mu_{N_0}}{\mu_{N_0+2}}}\langle R_{N_00}|r^2|R_{N_0+20}\rangle \tag{6}$$

$$M^{IS1} = \sqrt{3}\langle\Phi(1^-_{ex})|\mathcal{M}^{IS1}|\Phi(0^+_{gs})\rangle = \sqrt{\frac{3}{4\pi}}\left[\frac{3}{5}g_{N_0+3}\sqrt{\frac{\mu_{N_0}}{\mu_{N_0+3}}}\langle R_{N_00}|r^3|R_{N_0+31}\rangle \right.$$
$$\left. + g_{N_0+1}\sqrt{\frac{\mu_{N_0}}{\mu_{N_0+1}}}\left\{\frac{48}{25}\langle R_{N_00}|r^3|R_{N_0+11}\rangle + \frac{16}{3}\left(\langle r^2\rangle_\alpha - \langle r^2\rangle_{\rm O}\right)\langle R_{N_00}|r|R_{N_0+11}\rangle\right\}\right] \tag{7}$$

where $\langle r^2\rangle_\alpha$ and $\langle r^2\rangle_{\rm O}$ are the mean-square radius of the clusters. μ_N is the so-called eigenvalue of the RGM norm kernel. By using the amplitudes f_N and g_N calculated by AMD [19, 20], the formulae can be easily estimated as

$$M^{IS0} = 7.67f_{N_0+2} = 5.48\ {\rm fm}^2, \quad M^{IS1} = 3.08g_{N_0+1} - 7.36g_{N_0+3} = 5.82\ {\rm fm}^3, \tag{8}$$

which are as large as the Weisskopf estimates, $M^{IS0}_{\rm WU} = 6.37$ fm^2 and $M^{IS1}_{\rm WU} = 8.44$ fm^3. Thus, the IS monopole and dipole transitions to the cluster states are very strong. These strong transitions to the cluster states should be observed at relatively small excitation energies which are usually below the giant resonances, because the energies of the cluster states are governed by Ikeda threshold rule [24]. This explains why we have many narrow resonances well below the giant resonances. Therefore, the low-lying IS monopole and dipole strengths are the good signature of asymmetric clustering.

3. AMD results for ^{20}Ne, ^{44}Ti and ^{24}Mg

For the quantitative discussion, we have performed AMD calculations for several nuclei. Figure. 4 (a) shows the observed and calculated $\alpha + {}^{16}$O cluster bands in ^{20}Ne. The 0^+_4 and 1^-_1 states

IOP Conf. Series: Journal of Physics: Conf. Series **863** (2017) 012024 doi:10.1088/1742-6596/863/1/012024

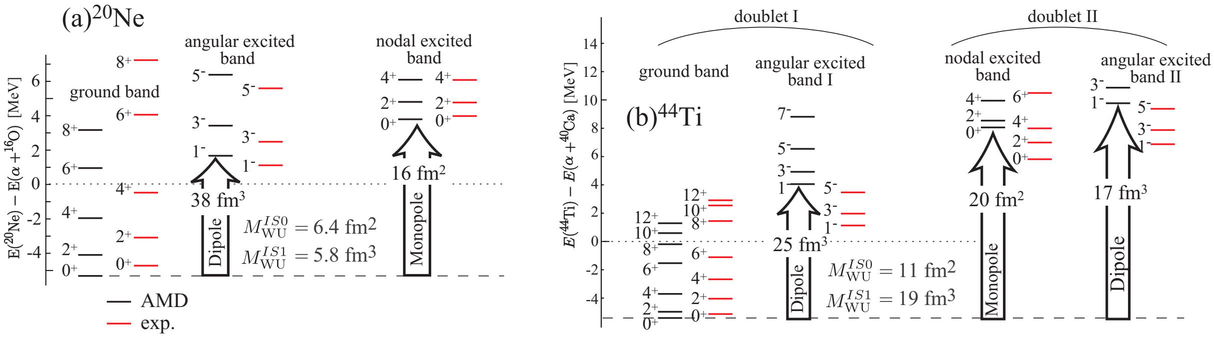

Figure 4. Observed and calculated (a) $\alpha + {}^{16}$O cluster bands in ^{20}Ne, and (b) $\alpha + {}^{40}$Ca cluster bands in ^{44}Ti. Arrows in the figure show the calculated transition matrices.

at 8.7 MeV and 5.8 MeV are identified as nodal and angular excited states [22], and AMD [19, 10] reasonably describes them. The calculated transition matrices are also shown in the figure. One sees that both of the IS monopole and dipole transitions are very strong and much more enhanced than the Weisskopf estimates and the cluster estimates given in Eq. (8). This enhancement owes to the $\alpha + {}^{16}$O clustering in the ground state.

Figure. 4 (b) shows the observed and calculated $\alpha + {}^{40}$Ca cluster bands in ^{44}Ti. The experimental assignment of the cluster bands is summarized as follows [25]. First, the ground state and the angular excited 1^- state at 6.2 MeV constitute a parity doublet denoted by "doublet I". Second, the nodal excited 0^+ state around 11 MeV and another angular excited 1^- around 12 MeV constitute another parity doublet denoted by "doublet II". AMD calculation [20, 10] reasonably reproduces them, although the excitation energies are slightly overestimated. As clearly seen in the figure, the transition strengths to these cluster states are as strong as the Weisskopf estimates as expected. However, they are not amplified as strong as in the case of ^{20}Ne. This is due to the reduction of the α clustering in the ground state of ^{44}Ti which is under the strong influence of the spin-orbit interaction. It is also noted that AMD calculation yields many other excited 0^+ and 1^- states below $E_x = 20$ MeV (not shown in Fig. 4 (b)), which do not have cluster structure. However, it was found that none of them have sizable IS monopole and dipole transition strengths. This suggests that these transitions are very sensitive and selective probe for the clustering. We also performed a similar analysis for ^{28}Si for which readers are directed to the contribution by Y. Chiba in this volume.

Figure. 5 shows the final example. Very high resolution data for IS monopole response of ^{24}Mg [17, 26] is available as shown by the histogram in the figure. The data shows the existence of the many narrow resonances below the giant monopole resonance. Solid lines shows the result of AMD calculation [21] which reasonably describes the distributions of the narrow resonances at small energy region as well as the giant resonance. From the analysis of the spectroscopic factor of AMD wave function, we can say that the resonance around 11 MeV is the $\alpha +^{20}$ Ne state, that at 13 MeV is the ^{12}C+^{12}C state and so on. Thus, the AMD calculations demonstrate that IS monopole/dipole transitions are excellent probe for the clustering.

4. Summary

In summary, we have discussed the relationship between the clustering and IS monopole/dipole transitions to demonstrate how and why they are excellent probe for clustering.

The Bayman-Bohr theorem tells us that the shell model states have duality of shell and cluster, and guarantees that the pronounced cluster states are populated by activating the degree-of-freedom of cluster excitation. This is a reason why the cluster states exist universally

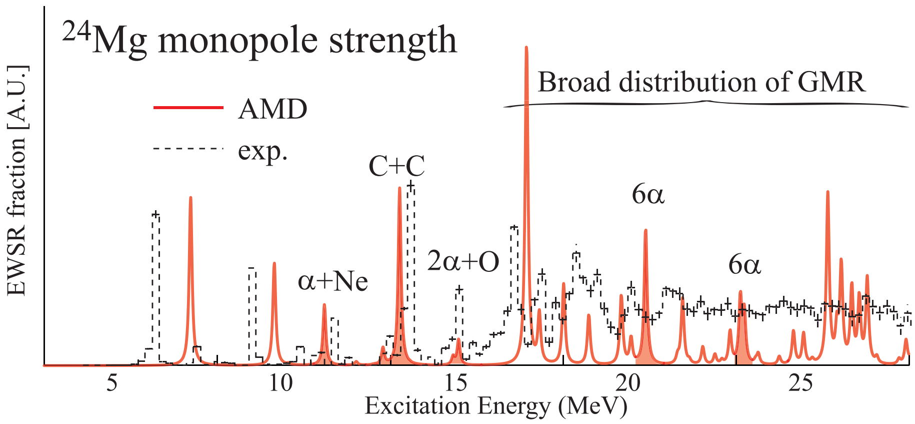

Figure 5. Observed and calculated IS monopole strength distributions of ^{24}Mg.

in atomic nuclei. The theorem is also utilized for deriving analytic formulae of the IS monopole/dipole transitions which show that these transitions do populate the cluster states very strongly.

The AMD calculations for ^{20}Ne, ^{44}Ti and ^{24}Mg are also presented. The results reasonably reproduce the known cluster states in ^{20}Ne and ^{44}Ti, and predict the transitions to the cluster states are very strong and selective. The results for ^{24}Mg is compared with the high resolution data. It is shown that by the analysis of the wave function, we can identify a variety of cluster states in ^{24}Mg such as $^{12}C+{}^{12}C$, $\alpha+{}^{20}Ne$ and $2\alpha+{}^{16}O$. Thus, the study of cluster states using IS monopole/dipole transitions is really fascinating and look promising.

References

[1] Wildermuth K and Kanellopoulos Th 1958 *Nucl. Phys.* **7** 150
[2] Wildermuth K and Kanellopoulos Th 1958/59 *Nucl. Phys.* **9** 449
[3] Bayman B F and Bohr A 1958/59 *Nucl. Phys.* **9** 596
[4] Elliott J P 1958 *Proc. Roy. Soc.* A **245** 128 and 562
[5] Perring J K and Skyrme T H R 1956 *Proc. Phys. Soc.* **69** 600
[6] Suzuki Y 1987 *Nucl. Phys.* A **470** 119
[7] Kanada-En'yo Y 2007 *Phys. Rev.* C **75** 024302
[8] Kawabata T *et al* 2007 *Phys. Lett.* C **646** 6
[9] Yamada T *et al* 2008 *Prog. Theor. Phys.* **120** 1139
[10] Chiba Y, Kimura M and Taniguchi Y 2016 *Phys. Rev.* C **93** 034319
[11] Youngblood D H, Lui Y W and Clark H L 1997 *Phys. Rev.* C **55** 2811
[12] Youngblood D H, Lui Y W and Clark H L 1998 *Phys. Rev.* C **57** 2748
[13] Lui Y W, Clark H L and Youngblood D H 2001 *Phys. Rev.* C **64** 064308
[14] Chen X *et al* 2009 *Phys. Rev.* C**80** 014312
[15] Itoh M *et al* 2011 *Phys. Rev.* C **84** 054308
[16] Itoh M *et al* 2013 *Phys. Rev.* C **88** 064313
[17] Gupta Y K *et al* 2016 *Phys. Rev.* C **93** 044324
[18] Peach T *et al* 2016 *Phys. Rev.* C **93** 064325
[19] Kimura M 2004 *Phys. Rev.* C **69** 044319
[20] Kimura M and Horiuchi H 2006 *Nucl. Phys.* A **767** 58
[21] Chiba Y and Kimura M 2015 *Phys. Rev.* C **91** 061302
[22] Tilley D R *et al* 1998 *Nucl. Phys.* A **636** 249
[23] Horiuchi H and Ikeda K 1968 *Prog. Theor. Phys.* **40** 277
[24] Ikeda K, Takigawa N and Horiuchi H 1968 *Prog. Theor. Phys. Supplement* Extra Number 464
[25] Yamaya T, Katori K, Fujiwara S, Kato S and Ohkubo S 1998 *Prog. Theor. Phys. Supplement* **132** 73, and references therein
[26] Kawabata T *et al* 2013 *Jour. Phys. Conf. Series* **436** 012009